Automatic and Quantitative Electroencephalographic Characterization of Drug-Resistant Epilepsy in Neonatal KCNQ2 Epileptic Encephalopathy

Zheng Zeng, Yan Xu, Chen Chen, Ligang Zhou, Yalin Wang, Minghui Liu, Long Meng, *Member, IEEE*, Yuanfeng Zhou, and Wei Chen, *Senior Member, IEEE*

***Abstract*— KCNQ2 epileptic encephalopathy is relatively common in early-onset neonatal epileptic encephalopathy and seizure severity varied widely, categorized as drug-sensitive epilepsy and drug-resistant epilepsy. However, in clinical practice, anti-seizure medicines need to be gradually adjusted based on seizure control which undoubtedly increases the economic burden of patients, so further positive anti-seizure regimens depend on whether seizure severity can be predicted in advance. In this paper, we proposed a reliable assessment to differentiate between drug-sensitive epilepsy and drug-resistant epilepsy caused by KCNQ2 pathogenic variants. Based on the electroencephalogram (EEG) and electrooculogram (EOG) signals, twenty-four classical temporal and spectral domain features were extracted and Gradient Boosting Decision Tree (GBDT) was employed to distinguish between patients with drug-sensitive epilepsy and drug-resistant epilepsy. In addition, we also systematically investigated the impact of channel combination and feature combination based on the forward stepwise selection strategy. By employing selected channels and features, the classification accuracy can reach 81.25% with a sensitivity of 57.14% and specificity of 100%. Compared with the state-of-the-art techniques, including the functional network, effective network, and common spatial patterns, the improvement of accuracy ranges from 37.5% to 56.25%, indicating the superiority of our proposed method. Overall, the proposed method may provide a promising tool to distinguish different seizure outcomes of KCNQ2 epileptic encephalopathy.**

***Index Terms*— KCNQ2 epileptic encephalopathy, drug-resistant epilepsy, electroencephalogram (EEG), gradient boosting decision tree (GBDT).**

I. Introduction

KCNQ2 is a confirmed epilepsy pathogenic gene, located on the long arm of chromosome 20, at position 13.3. KCNQ2 gene encodes the voltage-gated potassium channel subunits KV7.2 and is a key factor in regulating neural excitability [1]. Pathogenic variants on KCNQ2 gene may reduce the activation threshold of the neuron, leading to early-onset neonatal epilepsy or epileptic encephalopathy (EE) in neonates. In the clinic, KCNQ2 EE patients are all required to take ASM treatments continuously to reduce the frequency and severity of seizures. According to seizure outcome, patients who achieved sustained seizure-free with antiseizure medicines (ASMs) were diagnosed with drug-sensitive epilepsy (DSE), while those who failed to adequate trials of two ASMs were diagnosed as drug-resistant epilepsy (DRE) [2]. However, to diagnose the specific type of KCNQ2 EE (DSE or DRE), long-term ASM treatment and follow-up are required to determine whether ASM drugs have a positive therapeutic effect on KCNQ2 EE patients. This process is time-consuming and may greatly influence whether to adopt positive treatment regimens or not, for early and rational intervention is especially important for neonates to reach good outcomes. In addition, the miscategorization of DSE and DRE may cause unnecessary psychological and economic burdens, which also bring out a potential risk of inappropriate treatment or side effects. Thus, in our study, we attempt to identify the KCNQ2 EE patients in advance after initial ASMs treatments

Manuscript received 5 September 2022; revised 1 June 2023; accepted 3 July 2023. Date of publication 13 July 2023; date of current version 26 July 2023. This work was supported in part by the Shanghai Municipal Science and Technology International Research and Development Collaboration Project under Grant 20510710500, in part by the Shanghai Committee of Science and Technology under Grant 20S31903900, and in part by the National Natural Science Foundation of China under Grant 62001118. *(Zheng Zeng and Yan Xu contributed equally to this work.) (Corresponding authors: Chen Chen; Yuanfeng Zhou; Wei Chen.)*

This work involved human subjects or animals in its research. Approval of all ethical and experimental procedures and protocols was granted by the ethics committee of the Children's Hospital of Fudan University under Approval No. 2022-51.

Zheng Zeng, Ligang Zhou, Minghui Liu, and Long Meng are with the Center for Intelligent Medical Electronics, School of Information Science and Technology, Fudan University, Shanghai 200433, China (e-mail: Zceng20@fudan.edu.cn; 21110720086@m.fudan.edu.cn; 21110720113@m.fudan.edu.cn; lmeng18@fudan.edu.cn).

Yan Xu and Yuanfeng Zhou are with the Department of Neurology, Children's Hospital of Fudan University, National Children's Medical Center, Shanghai 201102, China (e-mail: xuyanfimmu@163.com; yuanfengzhou@fudan.edu.cn).

Chen Chen is with the Human Phenome Institute, Fudan University, Shanghai 201203, China (e-mail: chenchen_fd@fudan.edu.cn).

Yalin Wang and Wei Chen are with the Center for Intelligent Medical Electronics, School of Information Science and Technology, Fudan University, Shanghai 200433, China, and also with the Human Phenome Institute, Fudan University, Shanghai 201203, China (e-mail: 19110720062@fudan.edu.cn; w_chen@fudan.edu.cn).

Digital Object Identifier 10.1109/TNSRE.2023.3294909

by exploring potential differences in EEG signals. This early identification would help the physicians in making a more appropriate and precise therapeutic intervention, then further effort needs to be paid to predicting the severity of seizures.

Recently, to distinguish different seizure severity of epilepsy, various methods have been proposed. DRE is often associated with malformations of the brain regions. Magnetic resonance imaging (MRI) is widely used to identify patients with DRE. By applying density imaging [3], image feature extraction [4] and diffusion tensor imaging [5], possible structural abnormality can be quickly detected by techniques of MRI analysis. However, imaging of KCNQ2-related epilepsy was reported to be normal in most neonatal patients [6], then MRI-based methods cannot distinguish severity of KCNQ2-related epilepsy effectively. In addition, MRI equipment is expensive and needs professional maintenance, which is unavailable in underdeveloped areas. Thus, these above-mentioned flaws are not conducive to the application of MRI for distinguishing KCNQ2 EE.

In contrast, electroencephalogram (EEG) is another promising technique to study EE. Compared with MRI, EEG signals has the advantages of lower cost and convenient acquisition. Extracting signal features from EEG for brain disease analysis has been widely applied in seizure prediction, epilepsy identification, epileptic foci detection, etc. Shiao et al. [7] extracted muti-frequency band features (i.e., 6 different frequency bands) for seizure prediction from intracranial electroencephalogram (iEEG) and achieved a high sensitivity of about 90-100%. Xu et al. [8] extracted the spatial pattern features from the resting EEGs. 92% accuracy was achieved for classifying psychogenic nonepileptic seizures from epilepsy. Boonyakitanont et al. [9] employed EEG signals for epileptic seizure detection with temporal and spectral domain features (i.e., variance, energy, kurtosis entropy and wavelet coefficients, etc.). The specificity of 83% was achieved with a sensitivity of 70% using the LDA classifier. These studies revealed the potential of EEG signals in reflecting the physiological state of patients' brains. By extracting the temporal and spectral domain features, cerebral pathological information can be captured effectively for epilepsy analysis. Recently, several studies have also found that unique patterns were detected in the EEG of KCNQ2 patients with DRE. Buttle et al. [10] observed a unique pattern of focal pointed theta waves of lambdoid morphology. These pointed theta waves were observed in all subsequent recordings. Kato et al. [11] observed interictal burst-suppression or multiple focal spikes in neonatal-onset EE patients. Ghimatgar et al. [13] described a very frequent episodes pattern of spike or sharp wave discharges in conventional EEG. Previous studies provided a perspective that KCNQ2 EE can often cause EEG abnormalities. However, whether the physiological information implicitly contained in the EEG signals can distinguish the seizure severity of KCNQ2 EE has not been systematically investigated. Neonates spend two-third of their lives sleeping [13], [14]. Thus, the acquisition of sleep EEG is convenient for practical use. Inspired by these aforementioned studies, we hypothesized that the sleep EEG signals of neonates could be used to distinguish seizure severity of KCNQ2 EE. Specifically, the inter-ictal sleep EEG signals of neonates were selected for analysis.

To quantitatively analyze the electroencephalographic characteristics of KCNQ EE, twenty-four classical temporal and spectral domain features from previous works [15], [16], [17], [18], [19], [20], [21], [22], [23], [24], [25] were extracted. These features can reflect potential pathological information. Besides, the effect of channel selection and feature selection to propose a compact model were investigated. A forward stepwise selection method to find the optimal channel combination is proposed, which would potentially reduce the acquisition cost, computational complexity and enhance the performance. Furthermore, the quality of EEG features is highly associated with the epilepsy identification performance. Here, we employed the wrapper technique to continue reducing redundant features, which has several merits in practical application. Firstly, through feature dimensionality reduction, redundant features can be excluded to reduce the computer cost. Secondly, the optimal feature combination is conducive to eliminating noise error, leading to performance improvement. Last, based on the fixed optimal feature combination, the trained compact model is not prone to overfitting. We used the forward greedy stepwise selection strategy to search for the optimal feature combinations until the classification accuracy no longer increased.

Our objectivein this paper is to propose a reliable method to distinguish seizure severity of KCNQ2 EE, which may provide auxiliary diagnosis and avoid the time-consuming medication process and follow-up process. Specifically, temporal and spectral domain features were extracted to distinguish the potential pathological abnormalities between DSE patients and DRE patients. The contributions of the proposed method can be summarized as follows:

1) To quantitatively analyze the electroencephalographic characteristics of KCNQ2 EE, features that can reflect the temporal and spectral EEG dynamics were extracted. Meanwhile, with the wrapper technique, redundant features were eliminated to reduce the model complexity and the potential indicators for distinguishing the DSE and DRE were reserved.
2) In consideration of acquisition cost and computational efficiency, channel selection is performed by a forward stepwise selection approach. With the channel selection process, it would not only potentially reduce the setup time in the signal acquisition, but also lessen the computational complexity and improve the performance in further EEG signal processing.
3) Our proposed method was validated on a clinical dataset of KCNQ2 EE, and the highest accuracy value of 81.25% can be reached. To the best of our knowledge, this is the first study to explore the feasibility of EEG in distinguishing the DSE and DRE of KCNQ2 EE.

The rest of this paper is organized as follows. In Section II, we introduce the dataset and data preprocessing. The extracted features, data balance technique, and validation strategy are also described. The results are presented in Section III. In Section IV, we discuss the results and compare our results with other state-of-the-art techniques. In the last section,

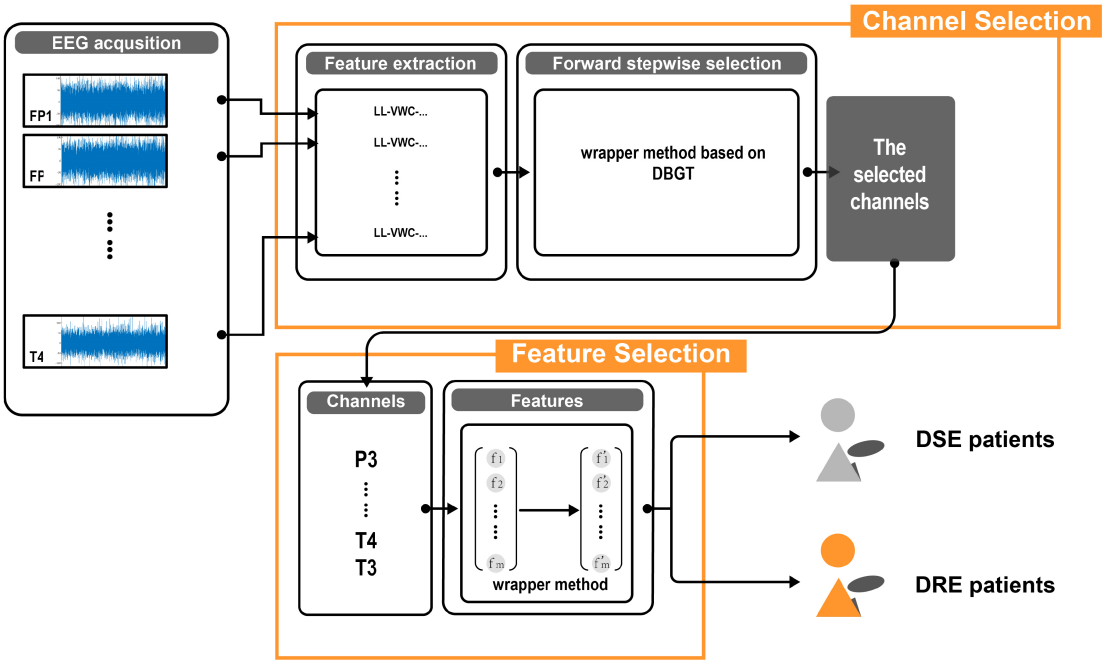

Fig. 1. The overall framework of the proposed method.

we conclude the paper and present the future work of this study.

II. Materials and Methods

The overall framework of the proposed approach includes the following stages: 1) Data acquisition, 2) Feature extraction and data balance, 3) Channels selection and feature selection, and 4) Classification. Firstly, we extracted the temporal and spectral features from each recorded channel. Secondly, a forward stepwise selection method was applied. Last, DSE patients and DRE patients were differentiated based on GBDT. The overall framework is shown in Fig. 1. And the details of each stage were elaborated as follows.

A. Dataset

A total of 20 neonatal patients with early-onset EE caused by KCNQ2 pathogenic variants were diagnosed by the physicians through clinical feature analysis and gene sequencing from 2016 to 2019. Patients were all required to take initial ASMs treatment to reduce the frequency and severity of seizures at first. After that, physicians needed to diagnose the patient's condition (DSE or DRE) according to the effect of long-term ASMs treatment and follow-up records. The specific diagnostic criteria were as follows: DSE: the success of adequate trials of two tolerated, appropriately chosen and used ASMs schedule. DRE: failure of adequate trials of two tolerated, appropriately chosen and used ASMs schedule [2].

After initial ASMs therapy, the EEG signals were collected by the Children's Hospital of Fudan University using the 10-20 system electrode locations. The electrode locations include F3, F4, T3, T4, C3, C4, P3, and P4. Meanwhile, two EOG channels namely EOG1 and EOG2 were also attached to record information of eye movements. The sampling rate was set to 500Hz with a 50Hz notch filter and a band-pass filter of 0.5Hz-70Hz. All the subjects were informed of the experiment's purpose and signed informed consent. This retrospective study was approved by the ethics committee of the Children's Hospital of Fudan University (approval number: 2022-51).

After EEG signals recording, the collected signals were labeled as different segments including seizures, body movements, wake and sleep by a senior neurophysiologist. Then, we selected the inter-ictal sleep epoch from patients for further analysis. Overall, sleep epochs of 16 patients (7 DSE patients and 9 DRE patients, 10 males and 6 females) were selected. The specific clinical information of patients with KCNQ2 EE is shown in Table I. The continued sleep EEGs signal were divided into five-second segments without overlap. Any segments affected by muscle movements or body movements were excluded. Ultimately, 3768 segments were selected from 16 patients for further analysis.

B. Feature Extraction and Data Balance Technique

In this study, we extracted twenty-four temporal and spectral domains features from the segments of each channel (as shown in Table II). These features were commonly used in epilepsy prediction and epilepsy classification, showing a reliable ability to recognize the pathological patterns of epilepsy [15], [16], [17], [18], [19], [20], [21], [22], [23], [24], [25]. Each feature was computed using the 5s segments. Features belonging to the same segment were concatenated to build a feature vector. For each channel, a 243768 feature matrix was obtained, accordingly. Let $x(t)$ be the 5s segment (a 5s segment contains N=2500 sampling points). The features can be calculated as follows:

TABLE I
CLINICAL INFORMATION OF PATIENTS WITH KCNQ2 EE

Patients	Gender	Date of hospitalization after birth	Date of Signal acquisition after initial ASM treatment	Date of KCNQ2 gene diagnosis after birth
DSE patient 1	Male	20 days	11 days	72 days
DSE patient 2	Male	21 days	19 days	222 days
DSE patient 3	Male	14 days	14 days	123 days
DSE patient 4	Female	25 days	14 days	108 days
DSE patient 5	Female	31 days	31 days	70 days
DSE patient 6	Male	9 days	9 days	85 days
DSE patient 7	Male	9 days	4 days	94 days
DRE patient 1	Male	20 days	17 days	46 days
DRE patient 2	Male	29 days	4 days	333 days
DRE patient 3	Female	6 days	11 days	73 days
DRE patient 4	Male	20 days	0 days	133 days
DRE patient 5	Female	5 days	1 days	89 days
DRE patient 6	Male	4 days	1 days	88 days
DRE patient 7	Female	15 days	1 days	96 days
DRE patient 8	Male	17 days	10 days	94 days
DRE patient 9	Female	11 days	0 days	128 days

-0 days: Signal acquisition and initial ASM treatment are at the same day.

1) Line length: Line length [15] is an effective feature in epilepsy analysis and can be defined as:

$$Linelength = \sum_{t=1}^{N} |x\,(t) - x\,(t-1)| \tag{1}$$

1) Wavelet-based features: Wavelet-based features [16] have been used in various epilepsy studies. Here, we extracted three wavelet-based features based on the Haar mother wavelet.

$$C(t)_b^a = \int x(t)\frac{1}{\sqrt{a}}\gamma(\frac{t-b}{a})dt \tag{2}$$

$$VWC = \frac{1}{N}\sum_{t=1}^{N}(C(t) - \bar{C})^2 \tag{3}$$

$$EWC = \frac{1}{N}\sum_{t=1}^{N}C(t)^2 \tag{4}$$

$$KWC = \frac{\frac{1}{N}\sum_{t=1}^{N}(C(t) - \bar{C})^4}{(\frac{1}{N}\sum_{t=1}^{N}(C(t) - \bar{C})^2)^2} \tag{5}$$

where $C(t)_b^a$ is the wavelet coefficient at scale a and position b. $\bar{C}$ is the average of the $C(t)$.

3) Hurst exponent: Hurst exponent [17] can reflect the tendency of time series. Here, we implement it based on the rescaled range analysis.

$$\lg\frac{R(N)}{S(N)} = \mathrm{HE} * \lg\mathrm{N} \tag{6}$$

where R(N) represents the cumulative range and S(N) represents the standard deviation. HE is the hurst exponent.

4) Sample entropy: Sample entropy [18] is a measurement of fluctuation in the time series, taking the following form:

$$SampEn(m,r) = \ln(\frac{\mathrm{K^{m+1}(r)}}{\mathrm{K^m(r)}}) \tag{7}$$

where m represents the embedding dimension and $r$is the tolerance. $\mathrm{K^m(r)}$ represents the probability of two sequences matching m points under tolerance r.

5) Mean: Mean value is the average of $x(t)$.

6) Coefficient of variation: Coefficient of variation reflects the data dispersion and is defined as the ratio of the standard deviation to the mean.

7) Mobility and complexity: Mobility and complexity represent the spectrum properties of EEG signals. Mobility [19] can be calculated as the ratio of standard deviation of the signal derivative to the standard deviation of the raw signal. Complexity [20] is the mobility of the signal derivative to the mobility of the raw signal.

8) Root mean square: Root mean square reflects the average power of the EEG signal which is given by the following form:

$$RMS = \sqrt{\frac{\frac{1}{N}\sum_{t=1}^{N}x(t)^2}{\mathrm{N}}} \tag{8}$$

9) Slope signal change: Slope signal change reflects the frequency information of EEG signal. The thresh is set to 40uv for all segments in this study.

10) Wavelength: Wavelength is the parameter reflecting both amplitude and frequency information. Let f_s be the sampling frequency. Wavelength is given by the following form:

$$WL = \frac{f_s}{\mathrm{N}-1}\sum_{t=1}^{N}|x(t) - x(t-1)| \tag{9}$$

11) Zero crossing: Zero crossing is an indicator of signal frequency. Its value is directly related to signal uncertainty.

TABLE II
THE 24 HAND-CRAFTED FEATURES

No.	*Features*	*Abbreviation*	*Parameters*
1	Line Length	*LL*	-
2	Variance Of Wavelet Coefficients	*VWC*	*Mother wavelet=Haar, scale=20*
3	Energy Of Wavelet Coefficients	*EWC*	*Mother wavelet=Haar, scale=20*
4	Kurtosis Of Wavelet Coefficients	*KWC*	*Mother wavelet=Haar, scale=20*
5	Hurst Exponent	*HE*	-
6	Sample Entropy	*SampEn*	-
7	Mean	-	-
8	Coefficient of Variation	*COV*	-
9	Mobility	-	-
10	Complexity	-	-
11	Root Mean Square	*RMS*	-
12	Slope Signal Change	*SSC*	-
13	Wavelength	*WL*	-
14	Zero-Crossing	*ZC*	-
15	Area Under Curve	*AUC*	-
16	Power spectra density of δ frequency band	*PSD of δ*	*segment overlap=50%, overlapped =8*
17	Power spectra density of θ frequency band	*PSD of θ*	*segment overlap=50%, overlapped =8*
18	Power spectra density of α frequency band	*PSD of α*	*segment overlap=50%, overlapped =8*
19	Power spectra density of β frequency band	*PSD of β*	*segment overlap=50%, overlapped =8*
20	Kurtosis	*Kurt*	-
21	Energy	-	-
22	Skewness	*Skew*	-
23	Variance	*Var*	-
24	Nonlinear Energy	*NE*	-

12) Area under curve: Area under curve (AUC) is calculated from the segments. We employed the trapezoidal rule to estimate the value of the integral.

13) Power spectral density of delta, theta, alpha, and beta frequency band [21]: the power spectral density was obtained by Welch's overlapped segment averaging estimator (Parameter: 50% segment overlap and 8 overlapped segments). If the length of the signal cannot be divided into an integer number of segments with 50% overlap, the signal is truncated accordingly.

14) Kurtosis: Kurtosis [22] is related to the sharpness of signal peak, which is given by the following form:

$$Kurt = \frac{\frac{1}{N}\sum_{t=1}^{N}(x(t)-\bar{x})^4}{\left(\frac{1}{N}\sum_{t=1}^{N}(x(t)-\bar{x})^2\right)^2} \tag{10}$$

15) Energy and variance: Energy [23] and variance [10] are the indicators related to the amplitude measurement. The detailed formulas are as follows:

$$Energy = \sum_{t=1}^{N} x(t)^2 \tag{11}$$

$$Var = \frac{1}{N}\sum_{t=1}^{N}(x(t)-\bar{x})^2 \tag{12}$$

16) Skewness: Skewness [24] is a digital feature of the degree of asymmetry of data distribution.

$$Skew = \frac{\frac{1}{N}\sum_{t=1}^{N}(x(t)-\bar{x})^3}{(\frac{1}{N}\sum_{t=1}^{N}(x(t)-\bar{x})^2)^{\frac{3}{2}}} \tag{13}$$

17) Nonlinear energy: Nonlinear energy [25] is sensitive to the high frequency oscillation, which can well capture the abrupt change in EEG signal.

$$NE = \sum_{t=2}^{N}(x(t)^2 - x(t-1)*x(t+1)) \tag{14}$$

In practical application, the dataset is often imbalanced due to distribution differences or sampling deviation. The difference in the number of signal segments of patients may lead the classifier to bias the learning results of the minority classes. Here, we employed Synthetic Minority Over-Sampling Technique (SMOTE) to balance the data for each training patient. SMOTE synthesizes new samples for minority classes based on interpolation. Compared with the technique of resampling the minority classes directly, it can prevent the generation of specific samples and the reduction of generalization. We performed the data balance technique on the training set and validated the performance on the remaining patient's data.

C. Channel Selection and Feature Selection

For the channel selection, we progressively increased the number of channels based on the forward stepwise selection strategy [26]. To be specific, the criterion in each forward step was that the selected channel contributed to the highest KCNQ2 patient recognition accuracy. We initially performed the evaluation with each channel and selected the channel satisfying the selecting criterion as the first selected channel. Then we separately combined the previously selected channel with each of the rest channels to evaluate the performance. The channel with the highest accuracy was selected and added to the optimal channel combination. The algorithm was terminated until all channels were selected. The optimal channel set was then determined based on the 10-round forward stepwise selection results.

The computational efficiency is highly dependent on the number of alternative features. Thus, it is not feasible to

directly optimize all features from all channels, which may cause computational burden or even dimension disaster. Excessive ineffective alternative features can also add the challenge of refining features. Hence, we further searched for the optimal feature combinations based on the selected channels. The forward greedy stepwise selection strategy was also applied in this process. Specifically, to obtain the optimal feature combination with the dimension of N_f, we gradually increased the number of features, via the wrapper technique from 1 to N_f.

D. Validation Protocol

The classification performance was evaluated by employing the Leave-One-Subject-Out-Cross-Validation. Namely, one patient's data was used as the test set and other patients' data was used as the training set. For each subject, we predicted the two types of KCNQ2 epileptic encephalopathy in lines with the most segments predicted type based on the hard voting method. To be specific, if more than 50% of the segments of a DSE (or DRE) patient are predicted to be DSE (or DRE), this DSE (or DRE) patient is considered to be classified correctly. We repeat the validation process until each patient's data has been used as the test set. The seven evaluation indices (accuracy, sensitivity, specificity, precision, recall, F1 score and kappa coefficients) were calculated as follows:

$$ACC = \frac{TP + FP}{N_{\mathrm{DSE}} + N_{DRE}} * 100\% \tag{15}$$

$$SEN = \frac{TP}{N_{\mathrm{DSE}}} * 100\% \tag{16}$$

$$SPE = \frac{TN}{N_{DRE}} * 100\% \tag{17}$$

$$PRE = \frac{TP}{TP + FP} \tag{18}$$

$$REC = \frac{TP}{TP + FN} \tag{19}$$

$$F1 = \frac{2 * PRE * REC}{PRE + REC} \tag{20}$$

$$p_0 = \frac{TP + TN}{N_{\mathrm{DSE}} + N_{DRE}},$$

$$p_c = \frac{(TP+FN) * (TP+FP) + (FP + TN) * (FN+TN)}{(N_{\mathrm{DSE}} + N_{DRE})^2}$$

$$K = \frac{p_0 - p_c}{1 - p_c} \tag{21}$$

where ACC, SEN, SPE, PRE, REC, F1 and K represent the accuracy, sensitivity, specificity, precision, recall, F1 score and kappa coefficients, respectively. TP and TN are the correctly identified number of DSE patients and DRE patients.FP and FN are number of wrongly identified DSE patients and DRE patients.N_{DSE} and N_{DRE} are the actual number of DSE patients and DRE patients, respectively.

E. Model Selection

To first select an optimal model, we systematically compared the baseline performance of Random Forests [27], Support Vector machine (SVM) [28], K Nearest Neighbor (KNN) [29], Naïve Bayes classifier (NB) [30], Linear Discriminant Analysis (LDA) [31], and Gradient Boosting Decision Tree (GBDT) [32] before channel selection and feature selection. The corresponding hyparameter combinations are listed in Table III. For each hyparameter combination, the accuracy was calculated for model evaluation. As shown in Fig.2, the GBDT achieved the best performance with an accuracy of 56.25%, outperforming all other models in classifying KCNQ2 patients. Based on this result, we selected and fixed the GBDT model for further analysis.

TABLE III
HYPERPARAMETER SETTING FOR THE CLASSIFIERS

Classifiers	Hyperparameters
RF	Estimator=50, 100, 150
SVM	Kernel = rbf, poly, and sigmoid
KNN	K=3, 5, 7, 9
NB	Var smoothing = $1e^{-9}$
LDA	Solver = svd and lsqr
GBDT	Trees = 200

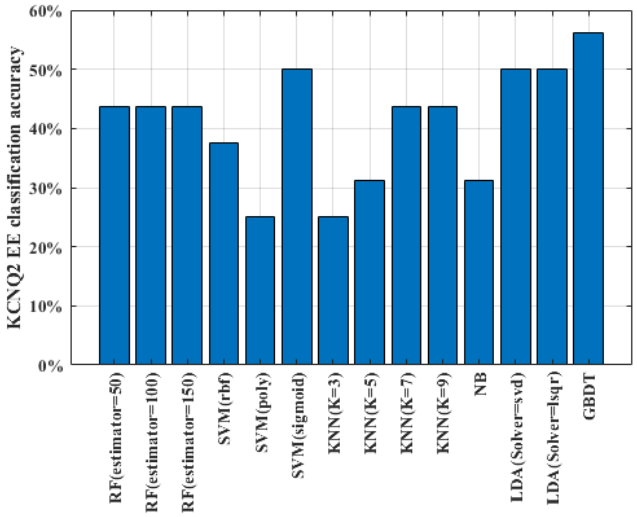

Fig. 2. Performance comparison of different classifiers.

III. RESULTS

A. Performance on Channel Selection

To differentiate the DSE patients and DRE patients, feature vectors were concatenated based on the forward stepwise selection strategy. The feature vectors were then fed into Gradient Boosting Decision Tree (GBDT) to identify the specific label of a patient. We conducted a total of 10 rounds of the channel selection process to find the optimal channel combination.

As shown in Table IV, the channel with the highest accuracy will be retained as the basis for subsequent selection. F3 channel was selected firstly and achieved an accuracy of 75% (SEN: 57.14% and SPE: 77.77%). In the second round, the SPE was further improved by adding the T4 channel. The

TABLE IV
CHANNEL SELECTION RESULTS BASED ON THE FORWARD STEPWISE SELECTION STRATEGY

Round	Added channel	ACC%	SEN%	SPE%	PRE%	REC%	F1	Kappa
1	F3	75.00	57.14	88.88	80.00	57.14	0.66	0.47
2	T4	75.00	42.85	100.00	100.00	42.86	0.60	0.45
3	**T3**	**81.25**	**57.14**	**100.00**	**100.00**	**57.14**	**0.72**	**0.60**
4	EOG1	75.00	57.14	88.88	80.00	57.14	0.66	0.47
5	C3	68.75	42.85	88.88	75.00	42.86	0.54	0.33
6	P4	68.75	42.85	88.88	75.00	42.86	0.54	0.33
7	EOG2	62.50	28.5	88.88	66.66	28.57	0.40	0.18
8	C4	62.50	28.5	88.88	66.66	28.57	0.40	0.18
9	F4	56.25	28.5	77.77	50.00	28.57	0.36	0.06
10	P3	56.25	28.5	77.77	50.00	28.57	0.36	0.06

TABLE V
THE SELECTED FEATURES COMBINATIONS AND RELATED ACCURACY

No.	Feature combination	ACC%	SEN%	SPE%	PRE%	REC%	F1	Kappa
1	COV (F3) + COV (T4) + HE (F3)	81.25	57.14	100.00	100.00	57.14	0.72	0.60
2	COV (F3) + COV (T4) + SampEn (F3)	81.25	57.14	100.00	100.00	57.14	0.72	0.60
3	COV (F3) + COV (T4) + Mean (F3)	81.25	57.14	100.00	100.00	57.14	0.72	0.60
4	COV (F3) + COV (T4) + SSC (F3)	81.25	57.14	100.00	100.00	57.14	0.72	0.60
5	COV (F3) + COV (T4) + AUC (F3)	81.25	57.14	100.00	100.00	57.14	0.72	0.60
6	COV (F3) + COV (T4) + PSD of β (F3)	81.25	57.14	100.00	100.00	57.14	0.72	0.60
7	COV (F3) + Kurt (T4)	75.00	57.14	88.88	80.00	57.14	0.66	0.47

optimal channel combination appeared in the third round by adding channel T3. ACC, SEN, and SPE can achieve 81.25%, 57.14%, and 100%, respectively. Subsequent channel selections failed to further improve performance. As expected, the specific channel combination achieved the best performance in ACC, SEN, and SPE, indicating the ability of these channels to distinguish DSE patients and DRE patients. To intuitively view the effect of channel selection, we visualized the channel selection process. The channel combination of F3, T4, and T3 achieved the best performance in forward stepwise selection.

B. Performance on Feature Selection

After the forward stepwise channel selection, we employed the forward stepwise feature selection to search for the optimal feature combinations. Here, 24 features were extracted separately from the selected channels (F3, T4, and T3). Totally, 72 features were systematically investigated based on the Gradient Boosting Decision Tree classifier. The feature selection was terminated until reaching the maximum accuracy.

By adopting the Leave-One-Subject-Out-Cross-Validation technique, seven groups feature combinations were obtained (as shown in Table V). In the process of feature searching, the feature combination may vary due to multiple locally optimal solutions. We recorded and traversed the branches of each local optimal solution until the classification accuracy no longer increased. The selected feature combinations were: COV (F3) + COV (T4) + HE (F3); COV (F3) + COV (T4) + SampEn (F3); COV (F3) + COV (T4) + Mean (F3); COV (F3) + COV (T4) + SSC (F3); COV (F3) + COV (T4) + AUC (F3); COV (F3) + COV (T4) + PSD of β (F3); COV (F3) + Kurt (T4). The 81.25% classification accuracy can be achieved. Among all feature combinations listed in Table V, COV (F3) and COV (T4) were selected most, indicating their superiority in distinguishing KCNQ2 EE.

IV. DISCUSSION

In the proposed method, we employed the twenty-four temporal and spectral domain features to classify the two types of KCNQ2 EE. To further improve the performance, we employed channel selection and feature selection techniques to minimize the impact of redundant features. Channel selection and feature selection have several merits for practical application. First, the selected channels can not only capture

TABLE VI
THE PERFORMANCE COMPARISON WITH THE STATE-OF-THE-ART METHODS

Methods	ACC%	SEN%	SPE%	PRE%	REC%	F1	Kappa	Number of channels (features)
Functional EEG network	43.75	0.00	77.77	0.00	0.00	0.00	-0.24	10 (22)
Effective EEG network	43.75	0.00	77.77	0.00	0.00	0.00	-0.24	10 (22)
Fusion of functional and effective network	25.00	0.00	44.44	0.00	0.00	0.00	-0.57	10 (44)
Common spatial patterns	25.00	14.28	33.33	16.67	12.50	0.14	-0.50	10 (20)
Our proposed method	**81.25**	**57.14**	**100.00**	**100.00**	**57.14**	**0.72**	**0.60**	**2 (3)**

the brain abnormalities but also shield the impact of invalid channels. Also, channel reduction and feature reduction are potential values in epileptic encephalopathy, as these will help to reduce the acquisition cost and system consumption.

A. Performance on Channel Selection

Regarding the channel selection, our results show that the best performance can be achieved by using the selected three channels. In the clinic, three channels are generally considered enough to cover the epileptic focus [33]. For some partial seizures, the seizure patterns never spread to more than 6 channels. Selecting all the channels may involve the channels without seizure manifestations, which are regarded as the noise for the classification. Furthermore, from Table IV, the highest performance (ACC, SEN, SPE, PRE, REC, F1 and Kappa) can be reached by using the three channels (F3, T4, and T3). It should be noted that despite these selected channels are not exactly the same as the focal channels for all KCNQ2 patients, the high performance can still be reached by using these selected channels. Possible explanations may fall into two parts. Firstly, Seizure symptoms are often associated with abnormal conduction direction of abnormal discharge [34]. Channels away from the epileptogenic foci may be more conducive to capturing the spread information of the abnormal discharges. In addition, the focal channels detect the earliest changes of EEG signal, but it is not confirmed that they also have a notable effect on detecting potential disease mechanisms. Secondly, based on the early EEG changes, neuroscientists identify the focal channels. Since the focal channels are more highly related to the seizures instead of the physiological abnormalities between KCNQ2 EE, the selected channels may not be exactly the same as these channels.

For the specifically selected channels (F3, T4, and T3), our results also show consistency with the reported cases of KCNQ2 EE. T4 and T3 channels are approximately located near the temporal regions. And the selected channel F3 is in the left frontal region. Previous case studies have reported that the clinical manifestations of most KCNQ2-related epilepsy show multiple focal spikes [35]. Part of the EEG phenotype in KCNQ2-related epilepsy shares the different unique discharge patterns (i.e., slow delta waves [36], frontal spikes [37], and harp waves over both temporal regions [35], [38]). Most of these patterns can be frequently observed in bilateral temporal regions and frontal regions. Thus, electrodes located in these areas are more sensitive to abnormal brain discharges, which may provide sufficient abnormal physiological information.

B. Performance on Feature Selection

Regarding the feature selection, we proposed the feature combinations to distinguish the DSE patients and DRE patients. By traversing the features from the selected channels, we obtained the seven group feature combinations. By using the selected features, ACC, SEN, and SPE gradually rose to convergence, which were sufficiently high compared with the accuracy when all the features were used. Thus, these feature combinations were recommended to distinguish pathological abnormalities.

For the wrapped feature selection strategy, different optimal feature subsets can be obtained based on different classifiers. Similarly, based on different feature selection approaches (filter, wrapper, and embedded approaches), the selected feature subsets can also vary from each other. Thus, the selected features may not have the explicit physiology significance but may achieve the best performance combined with the specific subset search strategy and subset evaluation approach [39]. The m best features may not be the best m features, because the m best features are most relevant to the classification, but there may be large redundancy between them [40]. Here, we investigated several feature combinations as shown in Table IV. Our work also demonstrated that temporal and spectral domain features from the EEG signals have the potential to detect different physiological abnormalities of KCNQ2 EE. Usually, EEG signals contained the abnormal discharge of neurons. Extracting relevant features from appropriate brain regions may further improve the performance of distinguishing KCNQ2 EE. Thus, advanced techniques to select appropriate channels and features are not only required for practical application but also for the improvement of accuracy.

C. Performance Compared With the State-of-the-Art Techniques

We also compared our work with state-of-the-art techniques. These techniques were: 1) Functional EEG network based on coherence. 2) Effective EEG network based on transfer

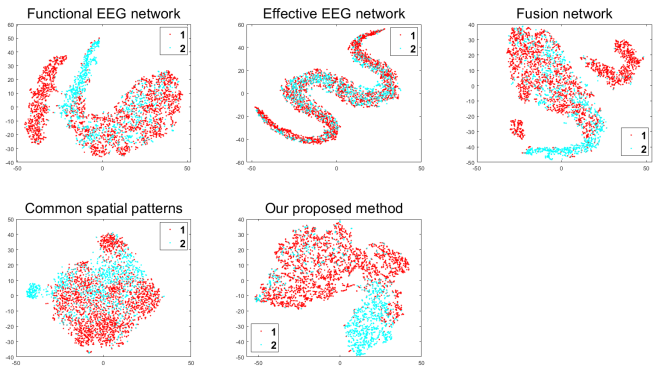

Fig. 3. The visualizations of KCNQ2 EE feature subspace. The red dots represent DSE sample points, while the cyan dots represent the DRE sample points.

entropy. 3) Common spatial patterns of functional and effective EEG networks. For the functional network and effective networks, the network properties including local efficiency, global efficiency, characteristic path length, and clustering coefficient were extracted for classification. All these network properties were calculated with the Brain Connectivity Toolbox [41]. As for the common spatial patterns, we employed the scheme in [42] to generate the spatial pattern of the network filters. The spatial patterns were extracted in the network space. To ensure fairness, all these techniques were implemented in our dataset.

Network properties have been used for the diagnosis of some neurological diseases in previous studies [43], [44], [45]. However, it is difficult directly distinguish the KCNQ2 EE based on the network properties as shown in Table VI. Neither the functional network, effective work, nor the combination of these two networks can reflect the pathological differences between the two different seizures of KCNQ2 EE. One possible explanation is that the four network properties based on graph theory analysis are the statistic measurements, which cannot fully represent all the potential information of the network. Abnormal information in the KCNQ2 EE may be more complicated than these network properties. Consequently, network properties cannot provide effective differentiation for patients with KCNQ2 EE.

Regarding the common spatial patterns of functional and effective networks, the performance was further degraded compared with the network properties. Commonly, the common spatial patterns can extract the spatial pattern of networks (SPN), which can reflect the connective strength of nodes and potential pathological differences underlying core brain regions. However, fusing spatial features among functional and effective networks may not be an effective approach to classify the two types of KCNQ2 EE compared with our proposed method. This can be explained from the following two perspectives. Firstly, the common space patterns are sensitive to different brain spatial modes. Thus, they are highly effective in distinguishing psychogenic nonepileptic seizures from epileptic seizures [8], or patients with schizophrenia from healthy controls [46]. Compared with these neurological diseases, it still remains uncertain whether there are significant differences in spatial patterns of networks among patients with KCNQ2 EE. Accordingly, the methods based on common spatial patterns may not provide a satisfactory differentiation of KCNQ2 EE. Secondly, the brain networks constructed by different methods may lead to performance differences. Thus, the brain network methods for KCNQ2 EE classification are still needed further exploration.

Regarding the results, it is noted that the sensitivity of all methods achieved a relatively low performance. Especially, the EEG network nearly can not distinguish the DSE patients. Here, we employed t-distributed stochastic neighbor embedding (t-SNE) to visualize the spatial distribution of local sample clusters (as shown in Fig.3). Regarding the state-of-the-art techniques, we found out that the sample distributions were similar between the two categories. The spatial distribution of features extracted by the SOTA methods is relatively close between DSE and DRE, showing high inseparability. Thus, the model may have difficulty distinguishing between DSE and DRE patients, resulting in extremely low metrics. As we visualized the temporal and spectral domains feature combinations, the sample distributions demonstrated high separability. However, compared with the DRE sample points, the DSE sample points were distributed with a larger intra-cluster variance. This may also leads the model to misclassify DSE as DRE, resulting in low evaluation metrics. Thus, the discriminative features are still needed a further exploration to separate the category samples of KCNQ2 EE in the feature space as far as possible.

D. Limitations

In this study, we demonstrated an EEG-based approach to distinguish between DSE and DRE for KCNQ2 EE. We correctly classified 13 out of the 16 patients. However, this work can still be enhanced via involving the following issues in our future work:

1) More EEG features can be extracted: Whether in the time domain, frequency domain, or time-frequency domain, these features have been used to analyze EE. More EEG-related features can be extracted to provide potential pathological abnormality, including high-dimension features extracted by a deep learning framework, which may provide discriminative and comprehensive information.
2) More KCNQ2 EE can be recruited: The number of patients in our dataset was relatively few. In this case, if one DSE (or DRE) patient is misclassified, the evaluation metrics may decrease significantly. However, the KCNQ2 patients are relatively rare and the data collecting is challenging. Although compared to related research, the data size used in this study can be generally considered as large, the absolute number of patients in each category is still not high. Nevertheless, our proposed approach is competitive compared with state-of-the-art techniques and demonstrate the feasibility of EEG in distinguishing KCNQ2 EE. In the future, we will extend the KCNQ2 EE dataset to propose a robust pathological analysis model.
3) More phenotypes of KCNQ2-related epilepsy can be considered: In this study, we distinguished two phe-

notypes of KCNQ2 EE (DSE and DRE). Additionally, KCNQ2 pathogenic variants cause benign epilepsy besides EE. It deserves a further investigation into whether our work is effective in distinguishing all these phenotypes.

V. Conclusion

In clinical practice, a long-duration is required to determine the response to ASMs and seizure outcomes of patients with KCNQ2 EE before providing further positive treatment regimens. It not only brings additional economic burdens and side effects, but also may affect early and rational intervention. In this work, an EEG-based approach to distinguish two different seizure outcomes in KCNQ2 EE was proposed. We extracted twenty-four temporal and spectral domain features from all the channels, respectively. By applying channel selection and feature selection techniques, we further reduced the acquisition cost and computational burden of the proposed approach. Ultimately, based on the only four selected features from the selected three channels, 13 out of the 16 KCNQ2 EE were correctly classified. Compared with the state-of-the-art approaches, our proposed method obtained higher accuracy while using fewer channels and features. Meanwhile, our proposed approach, combined with comprehensible features, can provide a promising tool to distinguish different seizure outcomes of KCNQ2-induced epileptic.

References

[1] J. J. Devaux et al., "KCNQ2 is a nodal K^+ channel," *J. Neurosci.*, vol. 24, no. 5, pp. 1236–1244, 2004.

[2] P. Kwan et al., "Definition of drug resistant epilepsy: Consensus proposal by the ad hoc task force of the ILAE commission on therapeutic strategies," *Epilepsia*, vol. 51, no. 6, pp. 1069–1077, 2011.

[3] M. Rostampour, H. Hashemi, S. M. Najibi, and M. A. Oghabian, "Detection of structural abnormalities of cortical and subcortical gray matter in patients with MRI-negative refractory epilepsy using neurite orientation dispersion and density imaging," *Phys. Medica*, vol. 48, pp. 47–54, Apr. 2018.

[4] Y. Fan et al., "Multivariate examination of brain abnormality using both structural and functional MRI," *NeuroImage*, vol. 36, no. 4, pp. 1189–1199, Jul. 2007.

[5] J. S. Duncan, "Imaging the brain's highways—Diffusion tensor imaging in epilepsy," *Epilepsy Currents*, vol. 8, no. 4, pp. 85–89, Jul. 2008.

[6] M. Milh et al., "Similar early characteristics but variable neurological outcome of patients with a de novo mutation of KCNQ2," *Orphanet J. Rare Diseases*, vol. 8, no. 1, pp. 1–8, 2013.

[7] H. Shiao et al., "SVM-based system for prediction of epileptic seizures from iEEG signal," *IEEE Trans. Biomed. Eng.*, vol. 64, no. 5, pp. 1011–1022, May 2017.

[8] P. Xu et al., "Differentiating between psychogenic nonepileptic seizures and epilepsy based on common spatial pattern of weighted EEG resting networks," *IEEE Trans. Biomed. Eng.*, vol. 61, no. 6, pp. 1747–1755, Jun. 2014.

[9] P. Boonyakitanont, A. Lek-uthai, K. Chomtho, and J. Songsiri, "A review of feature extraction and performance evaluation in epileptic seizure detection using EEG," *Biomed. Signal Process. Control*, vol. 57, Mar. 2020, Art. no. 101702.

[10] S. G. Buttle, E. Sell, D. Dyment, S. Bulusu, and D. Pohl, "Pointed rhythmic theta waves: A unique EEG pattern in KCNQ2-related neonatal epileptic encephalopathy," *Epileptic Disorders*, vol. 19, no. 3, pp. 351–356, Sep. 2017.

[11] M. Kato et al., "Clinical spectrum of early onset epileptic encephalopathies caused by KCNQ2 mutation," *Epilepsia*, 2013, vol. 54, no. 7, pp. 1282–1287.

[12] N. Kwak, Y. J. Lee, D. Kim, S.-K. Hwang, S. Kwon, and E. J. Lee, "KCNQ2 encephalopathy showing a distinct ictal amplitude-integrated electroencephalographic pattern," *Neonatal Med.*, vol. 27, no. 4, pp. 202–206, Nov. 2020.

[13] H. Ghimatgar et al., "Neonatal EEG sleep stage classification based on deep learning and HMM," *J. Neural Eng.*, vol. 17, no. 3, Jun. 2020, Art. no. 036031.

[14] M. Liu et al., "Overview of a sleep monitoring protocol for a large natural population," *Phenomics*, vol. 6, pp. 1–18, May 2023.

[15] R. Esteller R. Esteller, J. Echauz, T. Tcheng, B. Litt, and B. Pless, "Line length: An efficient feature for seizure onset detection," in *Proc. Conf. Proc. 23rd Annu. Int. Conf. IEEE Eng. Med. Biol. Soc.*, Oct. 2001, vol. 2, pp. 1707–1710.

[16] O. Faust, U. R. Acharya, H. Adeli, and A. Adeli, "Wavelet-based EEG processing for computer-aided seizure detection and epilepsy diagnosis," *Seizure*, vol. 26, pp. 56–64, Mar. 2015.

[17] H. E. Hurst, "Long term storage capacity of reservoirs," *Trans. Amer. Soc. Civil Eng.*, vol. 116, no. 1, pp. 770–799, 1951.

[18] J. S. Richman and J. R. Moorman, "Physiological time-series analysis using approximate entropy and sample entropy," *Amer. J. Physiol. Heart Circulatory Physiol.*, vol. 278, no. 6, pp. H2039–H2049, Jun. 2000.

[19] B. Hjorth, "EEG analysis based on time domain properties," *Electroencephalogr. Clin. Neurophysiology*, vol. 29, no. 3, pp. 306–310, Sep. 1970.

[20] M. Mursalin, Y. Zhang, Y. Chen, and N. V. Chawla, "Automated epileptic seizure detection using improved correlation-based feature selection with random forest classifier," *Neurocomputing*, vol. 241, pp. 204–214, Jun. 2017.

[21] K. Polat and S. Güneş, "Classification of epileptiform EEG using a hybrid system based on decision tree classifier and fast Fourier transform," *Appl. Math. Comput.*, vol. 187, no. 2, pp. 1017–1026, Apr. 2007.

[22] S. Ammar and M. Senouci, "Seizure detection with single-channel EEG using extreme learning machine," in *Proc. 17th Int. Conf. Sci. Techn. Autom. Control Comput. Eng. (STA)*, Dec. 2016, pp. 776–779.

[23] M. Li, W. Chen, and T. Zhang, "Classification of epilepsy EEG signals using DWT-based envelope analysis and neural network ensemble," *Biomed. Signal Process. Control*, vol. 31, pp. 357–365, Jan. 2017.

[24] P. Fergus, A. Hussain, D. Hignett, D. Al-Jumeily, K. Abdel-Aziz, and H. Hamdan, "A machine learning system for automated whole-brain seizure detection," *Appl. Comput. Inform.*, vol. 12, pp. 70–89, Jan. 2016.

[25] J. F. Kaiser, "On a simple algorithm to calculate the 'energy'of a signal," in *Proc. Int. Conf. Acoust., Speech, Signal Process.*, Apr. 1990, pp. 381–384.

[26] T. Alotaiby, F. E. A. El-Samie, S. A. Alshebeili, and I. Ahmad, "A review of channel selection algorithms for EEG signal processing," *EURASIP J. Adv. Signal Process.*, vol. 2015, no. 1, pp. 1–21, Dec. 2015.

[27] Z. Wang, D. Wu, F. Dong, J. Cao, T. Jiang, and J. Liu, "A novel spike detection algorithm based on multi-channel of BECT EEG signals," *IEEE Trans. Circuits Syst. II, Exp. Briefs*, vol. 67, no. 12, pp. 3592–3596, Dec. 2020.

[28] D. Wang et al., "Epileptic seizure detection in long-term EEG recordings by using wavelet-based directed transfer function," *IEEE Trans. Biomed. Eng.*, vol. 65, no. 11, pp. 2591–2599, Nov. 2018.

[29] M. Zeng, C. Zhao, and Q. Meng, "Detecting seizures from EEG signals using the entropy of visibility heights of hierarchical neighbors," *IEEE Access*, vol. 7, pp. 7889–7896, 2019.

[30] A. Page, C. Sagedy, E. Smith, N. Attaran, T. Oates, and T. Mohsenin, "A flexible multichannel EEG feature extractor and classifier for seizure detection," *IEEE Trans. Circuits Syst. II, Exp. Briefs*, vol. 62, no. 2, pp. 109–113, Feb. 2015.

[31] T. Zhang and W. Chen, "LMD based features for the automatic seizure detection of EEG signals using SVM," *IEEE Trans. Neural Syst. Rehabil. Eng.*, vol. 25, no. 8, pp. 1100–1108, Aug. 2017.

[32] D. Hu, J. Cao, X. Lai, J. Liu, S. Wang, and Y. Ding, "Epileptic signal classification based on synthetic minority oversampling and blending algorithm," *IEEE Trans. Cognit. Develop. Syst.*, vol. 13, no. 2, pp. 368–382, Jun. 2021.

[33] J. Duun-Henriksen, T. W. Kjaer, R. E. Madsen, L. S. Remvig, C. E. Thomsen, and H. B. D. Sorensen, "Channel selection for automatic seizure detection," *Clin. Neurophysiol.*, vol. 123, no. 1, pp. 84–92, Jan. 2012.

[34] R. Borgatti et al., "A novel mutation in KCNQ2 associated with BFNC, drug resistant epilepsy, and mental retardation," *Neurology*, vol. 63, no. 1, pp. 57–65, Jul. 2004.

[35] S. Weckhuysen et al., "KCNQ2 encephalopathy: Emerging phenotype of a neonatal epileptic encephalopathy," *Ann. Neurol.*, vol. 71, no. 1, pp. 15–25, Jan. 2012.

[36] I. C. Lee, M. Y. Chang, and J. S. Liang, "Ictal and interictal electroencephalographic findings can contribute to early diagnosis and prompt treatment in KCNQ2-associated epileptic encephalopathy," *J. Formosan Med. Assoc.*, 2021, vol. 120, no. 1, pp. 744–754, Jan. 2021.

[37] O. K. Steinlein, C. Conrad, and B. Weidner, "Benign familial neonatal convulsions: Always benign?" *Epilepsy Res.*, vol. 73, no. 3, pp. 245–249, Mar. 2007.

[38] J. Denis, N. Villeneuve, and P. Cacciagli, "Clinical study of 19 patients with SCN8A-related epilepsy: Two modes of onset regarding EEG and seizures," *Epilepsia*, vol. 60, no. 5, pp. 845–856, 2019.

[39] C. Lai, S. Guo, L. Cheng, and W. Wang, "A comparative study of feature selection methods for the discriminative analysis of temporal lobe epilepsy," *Frontiers Neurol.*, vol. 8, p. 633, Dec. 2017.

[40] H. Peng, F. Long, and C. Ding, "Feature selection based on mutual information criteria of max-dependency, max-relevance, and min-redundancy," *IEEE Trans. Pattern Anal. Mach. Intell.*, vol. 27, no. 8, pp. 1226–1238, Aug. 2005.

[41] M. Rubinov and O. Sporns, "Complex network measures of brain connectivity: Uses and interpretations," *NeuroImage*, vol. 52, no. 3, pp. 1059–1069, Sep. 2010.

[42] Y. Lin, P. Du, and H. Sun, "Identifying refractory epilepsy without structural abnormalities by fusing the common spatial patterns of functional and effective EEG networks," *IEEE Trans. Neural Syst. Rehabil. Eng.*, vol. 29, pp. 708–717, 2021.

[43] J.-R. Ding et al., "Altered functional and structural connectivity networks in psychogenic non-epileptic seizures," *PLoS One*, vol. 8, no. 5, May 2013, Art. no. e63850.

[44] H. Shen, L. Wang, Y. Liu, and D. Hu, "Discriminative analysis of resting-state functional connectivity patterns of schizophrenia using low dimensional embedding of fMRI," *NeuroImage*, vol. 49, no. 4, pp. 3110–3121, Feb. 2010.

[45] L.-L. Zeng et al., "Identifying major depression using whole-brain functional connectivity: A multivariate pattern analysis," *Brain*, vol. 135, no. 5, pp. 1498–1507, May 2012.

[46] F. Li et al., "Differentiation of schizophrenia by combining the spatial EEG brain network patterns of rest and task P300," *IEEE Trans. Neural Syst. Rehabil. Eng.*, vol. 27, no. 4, pp. 594–602, Apr. 2019.